Spring 2018

Modeling Effects of Rainwater Harvesting Systems on Water Yield Increase and Non-Beneficial Evaporation Reduction to Sustain Agriculture in a Water-Scarce Region of China

Tennille Wade
Old Dominion University, tennillebrandy@cox.net

MODELING EFFECTS OF RAINWATER HARVESTING SYSTEMS ON WATER YIELD INCREASE AND NON-BENEFICIAL EVAPORATION REDUCTION TO SUSTAIN AGRICULTURE IN A WATER-SCARCE REGION OF CHINA

by

Tennille Wade
B.S. May 2009, Old Dominion University
M.S. May 2018, Old Dominion University

A Thesis Submitted to the Faculty of
Old Dominion University in Partial Fulfillment of the
Requirements for the Degree of

MASTER OF SCIENCE

ENVIRONMENTAL ENGINEERING

OLD DOMINION UNIVERSITY
May 2018

Approved by:

Xixi Wang (Chair)

David Sample (Member)

Gary Schafran (Member)

Mujde Erten-Unal (Member)

ABSTRACT

MODELING EFFECTS OF RAINWATER HARVESTING SYSTEMS ON WATER YIELD INCREASE AND NON-BENEFICIAL EVAPORATION REDUCTION TO SUSTAIN AGRICULTURE IN A WATER-SCARCE REGION OF CHINA

Tennille Wade
Old Dominion University, 2018
Director: Dr. Xixi Wang

The northwestern region of China, which has an arid/semiarid climate, relies heavily on agriculture to provide food for the growing population. Climate change is affecting water availability in the region, causing long periods of drought and water scarcity followed by shorter periods of heavy rainfall and excess water availability. The ridge and furrow rainwater harvesting systems (RFRWHS) are a means of solving the problem of water scarcity; the systems can replenish soil moisture, reduce non-beneficial evaporation from bare soils, and increase surface water yield. In such a region, the hydrologic cycle is dominated by soil evaporation, leading to minimal surface runoff and depletion of soil water. For this thesis, hydrologic models were developed to predict the effects of the RFRWH systems on increases in water yield and reduction of non-beneficial evaporation. The results indicate that water yield will increase with increasing ridge width, and the systems with a common plastic mulch or biodegradable plastic mulch are most effective in increasing water yield. These two mulches may be good choices for increasing water availability and adapting to climate change. Potential evapotranspiration (PET) models are a tool used to measure non-beneficial evaporation. PET models results showed that PET tended to increase over the past several years, possibly due to climate change, while the average soil evaporation during the growing seasons (April to October) was reduced by 40% due to the RFRWH systems. This reduced soil evaporation may have increased the water available

for crops in the furrows, thus increasing crop yields. The percentage of precipitation lost to non-beneficial soil evaporation may have been reduced as much as 30% by using the RFRWH systems.

ACKNOWLEDGMENTS

To Dr. David Sample and Dr. Xixi Wang for their help throughout the semester in completing research and drafting this thesis. I appreciate their guidance and help. To my committee members, Dr. Mujde Erten- Unal, Dr. Xixi Wang, Dr. Gary Schafran and Dr. David Sample, your time and effort is appreciated greatly.

To Mr. Qi Wang thank you for providing so many resources from China at the Cold and Arid Region Environmental and Engineering Research Institute, Chinese Academy of Sciences, Gansu Agricultural University, The laboratory of Arid Agroecology, School of Life Sciences, and State Key Laboratory of Soil Erosion and Dryland Farming on Loess Plateau, Institute of Soil and Water Conservation.

Finally, to my family, thank you for giving me support, space and understanding. I would not have gotten this accomplished without you.

NOMENCLATURE

Q	Runoff (mm)
ET_o	Reference Evapotranspiration(mm/day)
e_a	Actual vapor pressure (kPa)
e_s	Saturation vapor pressure (kPa)
G	heat flux density to the ground (MJ/m^2d)
n	Actual duration of bright sunshine hour or maximum possible hours of sunshine
N	Max Possible duration of bright sunshine hour or maximum possible hours of sunshine
P	Atmospheric pressure (kPa)
R_a	Extraterrestrial radiation (mm/day)
R_e	Runoff Efficiency
R_s	Solar radiation (mm/day)
R_n	Net radiation (MJ/m^2d)
R_{ns}	Net Shortwave radiation (MJ/m^2d)
R_{nl}	Net Longwave radiation (MJ/m^2d)
T_{max}	Mean monthly air temperature (℃)
T_{min}	Mean air temperature, (℃)
u_2	Horizontal wind speed at height 2.0 m (m/s)
λ	Latent heat of vaporization (MJ/kg)
Δ	Slope of saturation vapor pressure temperature curve (kPa/℃)
γ	Psychometric constant (k. Pa/ ℃)
α	Albedo constant
θ	Soil moisture (mm)
Θ_{fc}	Field Capacity Soil moisture
θ_{wp}	Wilting Point Soil moisture
ω_s	Sunset angle (rad)
ϕ	Latitude (rad)
δ	Solar declination (rad)
h_1	Ridge width (cm)
h_2	Furrow width (cm)
w_1	Soil moisture before sowing
w_2	Mean soil moisture from ridges and furrows
d_r	Inverse relative distance between earth and sun

ACRONYMS

AMC	Antecendent Moisture Condition
BMR	Biodegradable plastic Mulch
CMR	Common plastic Mulch
CN	Curve Number
D	Deep seepage
E_{so}	Soil Evaporation
ET	Evapotranspiration
FAO	Federal Agriculture Organization
FPM	FAO Penman-Montieth
FY	Forage yeild
I	Infiltration
MoCN	Modified Curve Number
PET	Potential Evapotranspiration
RCM	Regional Climate model
RMSE	Root Mean Square Error
P	Precipitation
RWH	Rainwater Harvesting
RFRWH	Ridge and Furrow Rainwater Harvesting
SCS	Soil Conservation Service
SR	Soil crust
SW	Soil Water
T	Transpiration
WUE	Water Use Efficiency

TABLE OF CONTENTS

Page

NOMENCLATURE v

ACRONYMS vi

LIST OF TABLES viii

LIST OF FIGURES iix

Chapter

1. INTRODUCTION 1
   - 1.1 Problems and Research Needs 1
   - 1.2 Previous Studies 4
   - 1.3 Objectives 8
   - 1.4 Thesis Structure 9

2. MATERIALS AND METHODS 11
   - 2.1 Study Site 11
   - 2.2 Field Experiment 11
   - 2.3 Water Balance in the RFRWH 14
   - 2.3.1 Estimating ET 15
   - 2.3.2 Modeling runoff 17

3. RESULTS AND DISCUSSION 21
   - 3.1 The Calibrated model 21
   - 3.2 Simulated Water Yields of the RFRWH Systems 28
   - 3.3 Simulated Evapotranspiration 29
   - 3.4 Summary and Discussion 31

4. CONCLUSIONS AND RECOMMENDATIONS 33
   - 4.1 Conclusions 33
   - 4.2 Recommendation for future Research 35

REFERENCES 36

VITA 38

LIST OF TABLES

Table		Page
2-1	RFRWH system Plot descriptions	12
2-2	Definition of alfalfa growth stages	20
3-1	Adopted values of the model parameters	22
3-2	Summary of the models' performances	22
3-3	Annual simulated water yield results summary	29
3-4	Actual ET Hargreaves and FPM Potential ET model Results	30

LIST OF FIGURES

Figure		Page
1-1	Schematic of the RFRWH system	2
1-2	The RFRWH system with covered ridges and planted furrows	6
2.1	Location and land use of Gansu Province, China	11
2.2	RFRWH and FP Plot layout plan view	13
3.1	Modeled versus observed monthly runoff for: (a) SR30; (b) SR45; and (c) SR60	24
3.2	Modeled versus observed monthly runoff for: (a) CMR30; (b) CMR45; and (c) CMR60	25
3.3	Modeled versus observed monthly runoff for: (a) BMR30; (b) BMR45; and (c) BMR60	27

CHAPTER 1

INTRODUCTION

1.1 Problems and Research Needs

Water scarcity, in many developing countries, is a major problem for farmers and generally restricts growth of agriculture. Rainwater harvesting (RWH) is a method of collecting surface runoff during higher yielding rain periods and storing it in manmade or surface reservoirs. Stored water can provide needed water for potable uses, such as drinking water for people or livestock, or agricultural uses as irrigation water for crops (Helmrich and Horn 2008). The components of an agriculture water harvesting system include: runoff collection scheme, storage reservoir, catchment area, and planted area. The catchment area of the studied region referenced in this thesis has a runoff collection scheme that consists of a series of ridges and furrows (Fig 1-1), and the manmade storage reservoir consists of a series of 250 L buckets located on the downslope of the catchments ridges, and the furrows are the planted areas. The collection scheme is referred to as the ridge and furrow rainwater harvesting (RFRWH) system. Different land treatments (e.g., surface covers) influence the effectiveness of RWH by increasing or decreasing runoff. In practice, surface covers can be asphalt rubber, plastic, and/or mulches. For a given catchment, the most suitable land cover will be determined based on the catchment characteristics. The land cover materials for the study region of this thesis include common plastic mulch (CMR), biodegradable plastic mulch (BMR), and soil crust cover (SR). At a given site within the study region, the best land cover material for runoff production will be assessed based on the largest amount of runoff measured by a number of trial-and-error field experiments over several wet and dry weather cycles.

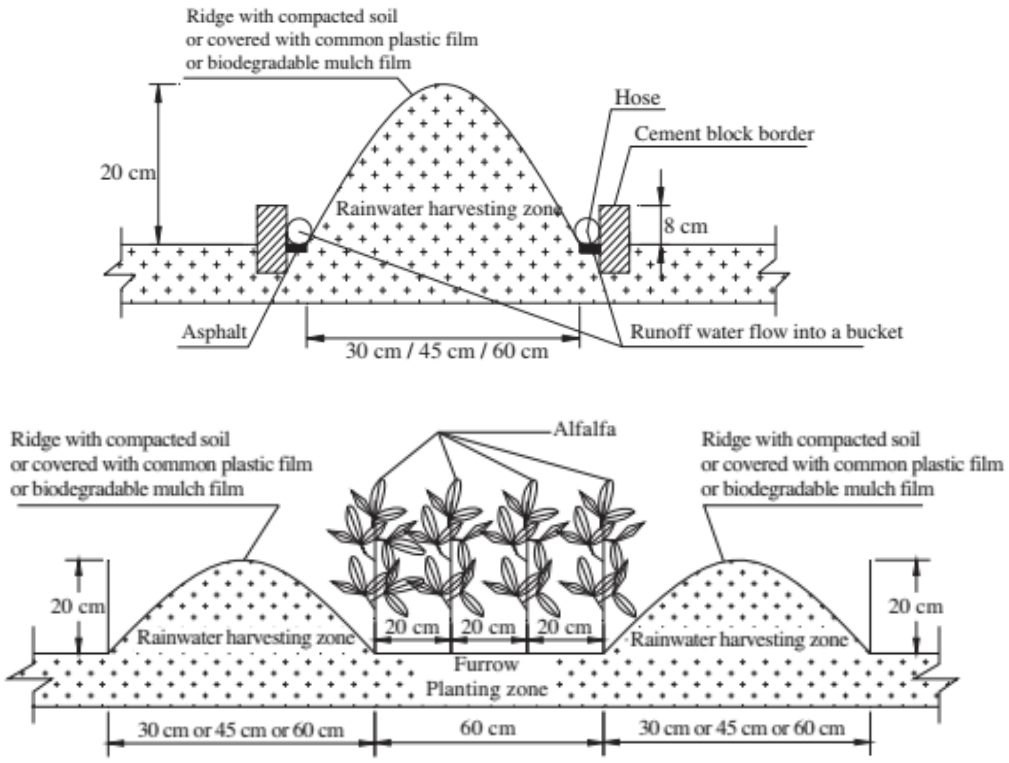

Fig 1-1. Schematic of the RFRWH system.

RWH has been widely practiced in arid/semiarid regions across the world for agricultural irrigation and/or soil-water replenishment (Adham *et al.* 2016). RWH practices increase crop yield by artificially manipulating evaporation and transpiration, which are dominant hydrologic processes in arid/semiarid environment, and by replenishing and sustaining soil water (Adham *et al.* 2016). A RWH reservoir is used to store rainwater generated from precipitation for utilization when it is needed, so RWH is an important supplement to conventional irrigation systems (e.g., irrigation canals and wells) when water supply is not enough to meet irrigation demand.

For a given RWH system, the major components of water balance include precipitation (P), evapotranspiration (ET), infiltration (I), and runoff (Q). In arid/semiarid regions, ET is the main process by which water is lost. Kumar *et al.* (2011) indicate that only 1% of P is used by plants while the remaining 99% is vaporized into the air to cool the plant and prevent

overheating. RWH practices are commonly designed to reduce ET by increasing the ratio of runoff to precipitation which is known as the runoff efficiency (R_e) and Q (Wang *et al*. 2015b). Thus, proper design of RWH systems requires a reliable model of the water balance components. Modeling in an ET-dominant and water-limited environment is a challenge for the hydrologic community due to variability of environmental factors affecting ET, such as temperature (T), P, humidity, and weather patterns. The sporadic nature of rainfall mandates that a hydrologic model be sensitive enough to capture the frequent wetting-drying cycles. Such a model is needed; however, few models of this type are documented in existing literature, in order to design and implement efficient RWH practices that minimize non-beneficial water loses (i.e. soil evaporation) while maximizing water use efficiency (WUE), defined as the ratio of biomass produced to the rate of transpiration (Wang *et al.* 2015b).

The effect of climate change on water resources is expected to play an important role in food production, primarily in grain growing areas (Misra, 2014). This is particularly true for regions such as Gansu Province located in northwest China, which has an arid/semiarid climate characterized by periods of frequent, sporadic, and short term heavy storm events usually followed by a long period of drought. Drought and extreme climates in arid/semiarid regions have become more serious with global warming (Wang *et al.* 2015b). The Yellow River is a major water source for Gansu Province, but its annual average runoff has decreased significantly in its middle reaches according to historical data recorded from 1957 to 2011 (Wang *et al.* 2015a). In many arid/semiarid areas, rain fed agriculture serves as a primary food source with approximately 90% of available land being used for food production (Helmreich and Horn, 2008). Agricultural productivity is closely related to the seasonal variability of precipitation and can be increased by optimizing the uptake efficiency of soil water. In arid/semiarid regions with

limited surface water, RWH may be the only cost-effective option for increasing rainwater efficiency and water supply. In this regard, RWH has been presented as a solution to water shortage problems in changing climate for decades (Shi *et al.* 2016).

1.2 Previous Studies

Agricultural rainwater harvesting is a type of RWH application with the objective of improving crop yield and production. As the sole source of water (i.e., inflow), P is converted into Q and/or soil water (SW), the change in soil water (ΔSW) is controlled by three processes:

1) evaporation from soil surface (Eso) and transpiration through crops (T),
2) runoff/runon from land surface, and
3) deep seepage through the bottom layer of soil profile (D).

T and Eso are usually combined into one term of evapotranspiration (ET). In an arid/semiarid environment, D is negligible due to a deep groundwater table (> 2 m), the regions topography with steep slopes, a low soil bulk density (1.38g/cm^3), and limited amount of water for deep percolation (Zhao *et al.* 2004). Thus, the water balance that governs the RWH system can be expressed as:

$$\Delta SW = P - Q - ET \quad (1\text{-}1)$$

Wang *et al.* (2015b) examined the effect of ridges and furrows on soil moisture, WUE, and runoff efficiency (R_e). The RFRWH system (Fig. 1-1) is a type of agricultural RWH practice that was developed to optimize the crop use efficiency of P by constructing a system of ridges and furrows. It increases Q from the ridges, which directs it into the furrows, where the water can be used by crops or collected/stored in reservoirs for irrigation when needed. Based on the two-year measurements, the authors found that the RFRWH system increased the R_e from 6 to 29% and effectively replenished the soil water by reducing soil water evaporation. Helmreich and

Horn (2008) reported that the annual potential ET (PET) in arid/semiarid regions varies from 1500 to 2300 mm, which is much larger than the corresponding annual precipitation and actual ET. The Actual ET is mainly satisfied by soil water evaporation (70 to 85%) and secondarily satisfied by transpiration (15 to 30%). During dormant seasons, Actual ET is fully satisfied by soil water evaporation.

The study conducted by Wang *et al.* (2015b) measured Q when the ridges of the RFRWH system were covered by SR, BMR, and CMR, to assess the influences of different covers on R_e, forage yield (FY), and WUE. The variations in ridge width and land treatment (Fig. 1-2) are signified by the following notations: Soil Crust ($SR^{30,45,60}$), common plastic mulch ($CMR^{30,45,60}$), biodegradable mulch ($BMR^{30,45,60}$), with the ridge bottom widths of 30, 45, and 60 cm noted as superscripts. The R_e was improved from 29% with the SR cover to 86% with the BMR cover, and to 88% with the CMR cover. The FY was affected most by the soil moisture, which was highest with the CMR cover and lowest with the SR. Soil moisture increased with the ridge width, P, and mulching material. Soil moisture closely followed rainfall fluctuations and was measured at its lowest during the first year of the study as an effect of high ET. R_e was highest when the width of the ridge was 60 cm and treated with the CMR, indicating CMR was the most efficient land cover material. The FY was consistently higher with the RFRWH system than what was typically observed over flat plains without a RFRWH system. The FY from the RFRWH plots was higher with the CMR cover than with the SR or the BMR cover. In contrast with soil moisture, the FY was higher for plots with a smaller ridge width regardless of the cover types (i.e. crop yield for $SR^{60} < SR^{45} < SR^{30}$). When the land treatments (SR, CMR, or BMR) were applied to the ridges, R_e, soil moisture, and FY were improved. The study demonstrated how effective the RFRWH practices were by showing improvement in soil moisture, R_e, and FY;

however, the authors did not develop a hydrologic model to generalize the systems' behavior limiting the evaluation and possible extension of the RFRWH practice to other similar areas.

Figure 1-2. The RFRWH system with covered ridges and planted furrows.

The Soil Conservation Service (SCS) Curve Number (CN) method is a method of estimating excess rainfall (i.e. runoff) from rainfall. The SCS-CN method and its modified

versions have been presented by Huang *et al.* (2005) and Wang *et al.* (2008). These modifications aimed to improve the prediction of Q by estimating CN as a continuous function of antecedent moisture condition (AMC), which is classified by the SCS into three categories, namely AMC_I, $AMC_{II,}$ and AMC_{III}. AMC_I reflects dry conditions, whereas, AMC_{III} reflects wet conditions. AMC_{II} is defined for normal conditions. In the conventional SCS-CN method, CN does not account for the dynamic process of wetting and drying of soils, resulting in sudden jumps of predicted Q. The modified version (MoCN) presented by Wang *et al.* (2008) continuously varies CN in terms of soil moisture between the CN for AMC_I (antecedent moisture condition at wilting point) and that for AMC_{III} (antecedent moisture condition at field capacity). On the other hand, Huang *et al.* (2005) examined influences of steeper (> 5%) overland slope on CN in the Loess plateau region of China. The authors hypothesized that with increase of slope, Q will increase while initial abstraction (I_a), infiltration and overland flow times will decrease. Herein, this thesis used the MoCN with CN adjusted by overland slope.

The examination of ET primarily relies on various climate models, such as Regional Climate Models (RCMs) (Feser *et al*. 2011). ET reflects water loss to the ambient atmosphere, while the water demand of plants plays a key role in estimating transpiration for the purposes of water management, irrigation planning, and other practices pertinent to agricultural production. Many studies have examined factors affecting ET and its spatiotemporal trends as an important indicator of climate change (Shi *et al*. 2016). The ET in many arid/semiarid areas tends to increase with aridity, making RWH practices more valuable in such areas (Su *et al.* 2015). The FAO Penmon Montieth method and Hargreaves method are the most common methods for estimating ET and were used in this study.

The performance of hydrologic model can be measured using Root Mean Square Error

(RMSE), expressed as:

$$RMSE = \sqrt{\frac{1}{N}\sum_{i=1}^{N}(Q_{obs} - Q_{comp})_i^2} \quad (1\text{-}2)$$

Where, Q_{obs} is the observed value of ruonff; Q_{comp} is the model value (Mishra *et al.* 2004). The value of the RMSE is an indicator of model performance, and the higher the value the poorer the models' performance with and RMSE of zero meaning a perfect fit of the model and observed data.

1.3 Objectives

In the Gansu Province of northwest China, average annual precipitation is 388 mm; 60% of which occurs between June and September, the time period when most crops have passed the key stage of requiring water at the beginning of their growth (Wang *et al*. 2015b). Approximately 65% to 69% of rainfall produces only 5 mm of P which is insufficient to provide for agricultural needs. Generally, the crops in the region need P of 10 mm or more for growth or for soil to maintain soil moisture conditions exceeding the wilting point. The nature of the arid/semiarid climate is that the time of year when rainfall events produce 10 mm or more of P is during the months corresponding with the dormant growth season. Water losses, through ET and Infiltration, negatively influence the soil water available for crops, resulting in either a smaller crop yield or a shorter growth season (Wang *et al*. 2015b). The hydrologic behavior, dominant hydrologic processes, and efficiency of the RFRWH system can be predicted by modeling the water balance. Further, the model can be implemented for developing better irrigation practices to improve agricultural production in changing climate.

ET is difficult to quantify; however, mathematical models have been developed to estimate the quantity of water loss due to ET. Previous studies estimated ET by using the FY of a

specific crop (Wang *et al*. 2015b). The Federal Agriculture Organization (FAO) published a report (Allen *et al*. 2006) that outlines a standard approach to model ET using the FAO Penman-Montieth (FPM) method. The Hargreaves equation can also be used for modeling ET, when limited environmental information is available. For this research, a water balance model was applied to a 41m^2 field in Gansu Province, China to evaluate the RFRWH system studied by Wang *et al.* (2015b).

Arid/semiarid regions face a unique challenge of having to keep up with growing populations and declining water availability due to climate change (Wang *et al*. 2015b). Climate change also influences the land available for planting crops, erosion and desertification resulting from unstable soils eroding under the influence of heavy bouts of rain after a long period of drought. Agriculture sustainability is a concern for people living in these areas. The RFRWH system can improve water availability by storing excess water for use during times of drought. The Q produced with RFRWH exceeds that produced without such a system; however, it is necessary to determine, through a hydrologic model, changes in soil water (ΔSW) that are crucial for crop growth.

The objectives of this thesis were to:

- Develop a hydrologic model that can be used to design/analyze RFRWH;
- Use the model to determine the effects of a RFRWH system on water supply; and
- Use the model to predict possible impacts of climate change on crop growth.

1.4 Thesis Structure

This thesis is based on data from 2012 to 2016. The project description and research conducted along with objectives of this work are presented in Chapter 1. Chapter 2 summarizes all data collected during the study period along with a description of how the data were collected

and a description of the study site and experiments conducted in the field. Chapter 2 also provides equations used in modeling Q and ET. Chapter 3 presents model calibration practices and the results of the model for Q and ET. Chapter 3 also summarizes and discusses the modeled variables for Q and ET and results. Chapter 4 provides a summary and makes recommendations for future research efforts.

CHAPTER 2

MATERIALS AND METHODS

2.1 Study Site

The study site (35°35'N, 104°37'E) (Fig. 2-1) is located at the Dingxi Arid Meteorology and Ecological Environment Experimental Station, operated by the Institute of Arid Meteorology of China Meteorological Administration. The climate of the site is characterized by moderate temperatures, with an annual average 7.2° C, a monthly maximum of 25.9°C in July and a monthly minimum of -13.0°C in January. The instantaneous maximum temperature was 33.8°C and the instantaneous minimum temperature reached -22.6°C. The average annual precipitation is 388 mm (Wang *et al.* 2015b). Soil at the site is Loess-like Loam having a wilting point of θ_{wp} = 6.7% and a water holding capacity of θ_{fc} = 25.6% for the 140 cm deep soil profile (Wang *et al.* 2015b).

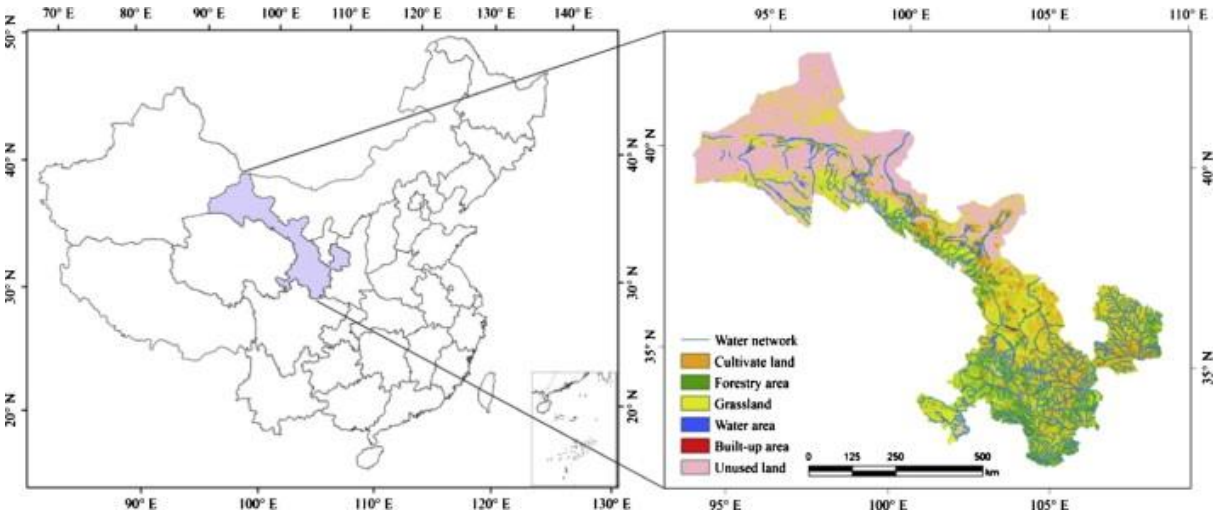

Fig. 2-1. Location and land use of Gansu Province, China.

2.2 Field Experiment

The study site consists of 30 plots that contain a series of ridges and furrows. Runon in

mm (Q_{on}) from the surrounding ridges, soil moisture in mm (θ), soil temperature in ^{0}C, and forage yield in kg ha^{-1}(FY) were measured for each plot. Individual plots contain four ridges and three furrows with 4 rows by 24 rows of planted alfalfa (Fig. 2-2). The furrow/planted area per plot was 18 m^2 (0.6 m width x 10 m depth x 3 furrows per plot =18 m^2). The ridge width, measured at the base of the ridge, varied; nine plots had ridges with 30 cm width, nine plots had ridges with 45 cm width, and nine plots had ridges with 60 cm width (Table 2-1). The ridge area per plot was 12 m^2 for the 30 cm ridge width, 18 m^2 for 45 cm ridge width, and 24 m^2 for 60 cm ridge width. The control plot (FP) had an area 36 m^2 (3.6 m width × 10 m length) and was planted with alfalfa. Of the 30 plots, including three control plots (FP), 27 were covered with land treatments. The FP plots were not; instead, alfalfa was planted without land treatment. The plot number and other properties associated with each plot are summarized in Table 2-1. There were three BMR, three CMR and three SR plots separated into ridge width: three BMR^{30}, three BMR^{45}, three BMR^{60}, three SR^{30}, three SR^{45}, three SR^{60}, three CMR^{30}, three CMR^{45}, and three CMR^{60} the layout of the plots, over the study site, was completely random. The meanings of these abbreviations are referenced in Chapter 1.

Table 2-1 RFRWH system plot descriptions[1].

Plot Numbers	Land Treatments	Furrow: Ridge (cm:cm)	Area of the ridge (m^2)	Area of the plot (m^2)	Area of the furrow (m^2)	Mulch Material
8, 14, 28	SR^{30}	60:30	12	30	18	Soil crust
9, 16, 30	SR^{45}	60:45	18	36	18	
7, 15, 29	SR^{60}	60:60	24	42	18	
3, 20, 27	BMR^{30}	60:30	12	30	18	Biodegradable
1, 18, 26	BMR^{45}	60:45	18	36	18	
2, 19, 25	BMR^{60}	60:60	24	42	18	
5, 11, 22	CMR^{30}	60:30	12	30	18	Common Plastic
4, 12, 21	CMR^{45}	60:45	18	36	18	
6, 13, 23	CMR^{60}	60:60	24	42	18	

[1]Alfalfa plantings were located within the furrows at 0.20 m centers for the width of the furrow and 1.6 m on center for the length of the furrow

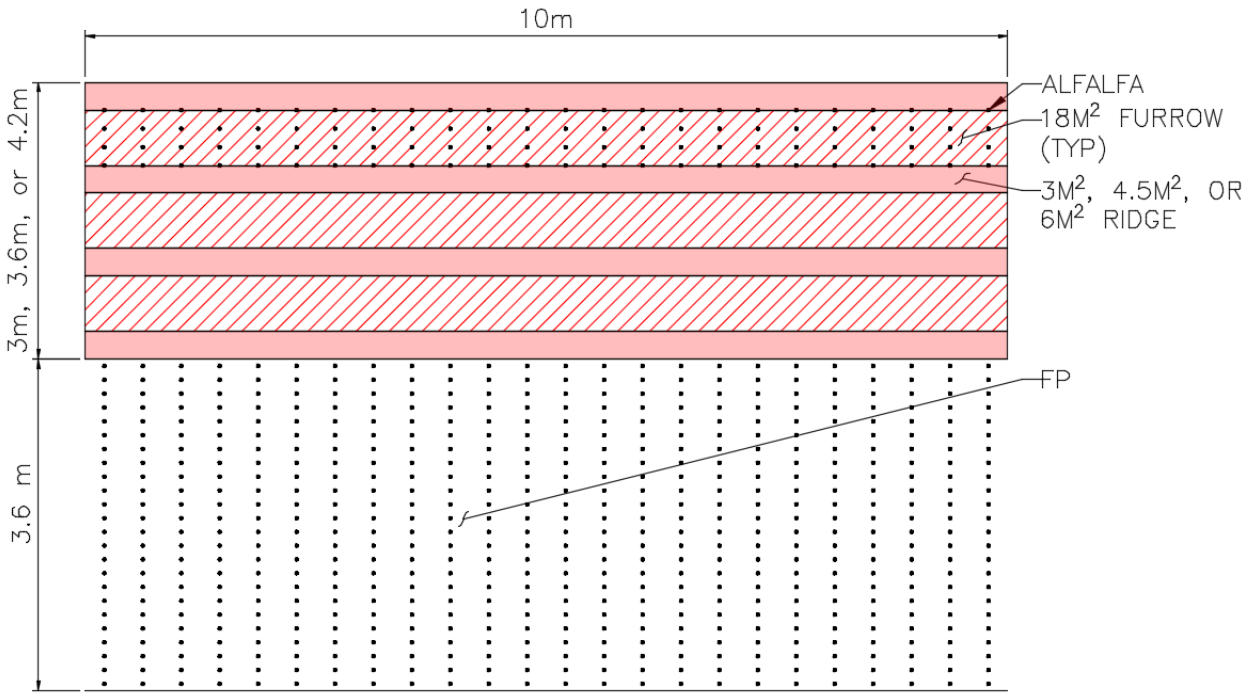

Fig. 2-2. RFRWH and FP Plot Layout Plan View.

Runon (Q_{on}), soil moisture (θ), soil temperature and forage yield (FY) information were measured at each of the plots, as specified here. Hereinafter, for a given plot, its water yield or runoff was almost the same as Q_{on} from its two ridges, so these three terminologies are interchangeable. Q_{on} was measured after each rain event by collecting it in 250 ml covered buckets placed downslope of each furrow. Each bucket was connected to hoses placed along each side of the ridge bottom (Fig. 1-1). Q_{on} was expressed as a depth (mm) by dividing the volume of Q_{on} in the bucket by the area of the respective ridge resulting in a depth for each event. Soil moisture was measured every ten days during the growing season (April through October) and after a rain event of 5 mm or more. Soil moisture measurements were made by weighing soil samples after collection, then weighing them again after oven drying to determine gravimetric water content. Then, the volumetric soil moisture was calculated by multiplying the gravimetric water content by bulk density (1.38 g/cm^3). Soil temperature was

measured using a set of mercury glass geo-thermometers placed at the furrow bottoms and ridge tops, recording soil temperature every 5 days starting at sowing (April) and ending at final harvest (October) three times (8:00 am, 2:00 pm and 6:00 pm) each day and at depths below the 5, 10, 15, 20, and 25 cm soil profiles. The measurements for these variables were recorded during two growing seasons in 2012 and 2013 and provided the basis to demonstrate the effectiveness of RFRWH. The conclusion of the 2015 study was that the most effective ridges which yielded the greatest FY and Q_{on} were CMR^{60} and BMR^{60} (Wang *et al.* 2015b).

2.3 Water Balance in the RFRWH

Development of a site water balance begins with identification of the dominant hydrological processes. Actual ET, as defined in (Eq. 2-1), is the sum of growing season precipitation (P), the ratio of ridge width to furrow width (h_1/h_2), ridge runoff efficiency (Re), and the difference between soil moisture measured in 200 cm depth one day prior to sowing (W_1), and the mean soil moisture value from furrow and ridges with common land treatments (CMR, BMR and SR) (W_2) (Wang et *al*. 2015b). That is, ET is computed as:

$$\mathrm{ET} = \mathrm{P} + \mathrm{Re} \times \mathrm{P} \times \frac{\mathrm{h_1}}{\mathrm{h_2}} + (\mathrm{W_1} - \mathrm{W_2}) \qquad (2\text{-}1)$$

The actual ET and Alfalfa FY define the water use efficiency (WUE) (Eq. 2-2). Alfalfa FY was determined using two approaches: forage yield (FY_1) based on furrow areas and FY_2 was based on land areas of ridges and furrows. FY_2 was generally the greater of the two values. The RFRWH system improves WUE and FY, and the design of the RFRWH was determined from the ridge with the highest WUE and FY.

$$WUE = \frac{FY}{ET} \qquad (2\text{-}2)$$

Data collection, in the field, for Q_{on} and actual ET, form the basis of the water balance

model. The models for Q_{on} and potential ET result in a linear regression equation and root mean square error RMSE (Eq. 1-1), respectively, which are used to evaluate model performance and validity. In this thesis, a modified version of the SCS-CN method, the MoCN method (Wang et al., 2008), is used to predict Q_{on}, while the Hargreaves method and the FAO Penman-Montieth (FPM) equation are used to predict potential ET.

2.3.1 Estimating ET

The Hargreaves (Hargreaves and Allen 2003) method for calculating potential ET (mm/day) is expressed as:

$$ET_0 = 0.0023(\text{Ra})(T + 17.8)(T_{max} - T_{min})^{0.5} \quad (2\text{-}3)$$

where T = the temperature in degrees Celsius and Ra = extraterrestrial radiation in $(\frac{MJ}{m^2 day})$(Allen $et\ al.$ 2006).

$$\text{Ra} = \frac{24(60)}{\pi} G_{sc} d_r [\omega_s \sin(\varphi)\sin(\delta) + \cos(\varphi)\cos(\delta)\sin(\omega_s)] \quad (2\text{-}4)$$

where G_{sc} = solar constant, or $0.0820\frac{MJ}{m^2 min}$; and d_r = inverse relative distance between the Earth and the Sun.

$$d_r = 1 + .033\cos(\frac{2\pi}{365}J) \quad (2\text{-}5)$$

where J = Julian day, and ω_s = sunset hour angle (rad).

$$\omega_s = arcos[-\tan(\varphi)\tan(\delta)] \quad (2\text{-}6)$$

where, ϕ = latitude (rad); and δ = solar declination (rad).

The FPM equation as described in Federal Agriculture Organization paper 56 (Allen *et al.* 2006):

$$\text{ET}_o = \frac{0.408\,\Delta(R_n - G) + \gamma\frac{900}{T+273}u_2(e_s - e_a)}{\Delta + \gamma(1 + .34u_2)} \quad (2\text{-}7)$$

where ET_o = reference evapotranspiration (mm/day); Δ = slope of saturation vapor pressure curve (kPa/ ^oC)(2-8); R_n = net radiation at the crop surface (MJ/m^2 day); G = soil heat flux density (MJ/m^2 day) (usually taken as zero for computing ET_o); γ = psychrometric constant (kPa/^oC)(2-14); T = air temperature (^oC); u_2= wind speed measured at 2 m above ground (m/s); e_s = saturation vapor pressure (kPa); e_a = actual vapor pressure (kPa); e_s - e_a = saturation vapor pressure deficit (kPa).

Δ is computed as:

$$\Delta = \frac{4098[0.6108e^{\frac{17.27T}{T+273.3}}]}{(T+273.3)^2} \quad (2\text{-}8)$$

R_n is defined as the difference between net shortwave radiation, R_{ns}, and net longwave radiation, R_{nl}. R_{ns}, is computed as:

$$R_{ns} = (1-\alpha)\, R_s \quad (2\text{-}9)$$

where α = albedo or canopy reflection coefficient (usually 0.23 for agricultural lands), and R_s = solar radiation (MJ/m^2 day).

$$R_s = \left(0.25 + 0.50\frac{n}{N}\right) R_a \quad (2\text{-}10)$$

where n = actual duration of sunshine (hours), and N = max possible duration of sunshine or daylight (hours).

$$N = \frac{24}{\pi}\omega_s \quad (2\text{-}11)$$

R_{nl} is computed as:

$$R_{nl} = 4.903\text{x}10^{-9}\left[\frac{Tmax.K^4 + Tmin,K^4}{2}\right]\left(0.34\text{-}0.14\sqrt{e_a}\right)\left(1.35\frac{Rs}{Rso}\text{-}0.35\right) \quad (2\text{-}12)$$

where R_{so} = clear sky solar radiation (MJ/m^2 day); $T_{max,K}$ = maximum temperature (K); and $T_{min,K}$ = minimum temperature (K); e_a = actual vapor pressure (kPa).

R_{so} is computed as:

$R_{so} = (0.75+2\times10^{-5}z)R_a$ (2-13)

where z = station elevation above sea level (m). Herein, it is 1896.7 m. G = soil heat flux density (MJ/m^2 day) (taken as zero for computing ET_o); γ = psychrometric constant (kPa/^oC).

γ is computed as:

$$\gamma = 0.665x10^{-3}\left[101.3(\frac{293-0.0065z}{293})^{5.26}\right] \quad (2\text{-}14)$$

where u_2= wind speed measured at 2 m above ground (m/s); e_s = saturation vapor pressure (kPa).

e_s is computed as:

$$e_s = \frac{0.611e^{\frac{17.27\,T_{min}}{T_{min}+273.3}}+0.611e^{\frac{17.27\,T_{max}}{T_{max}+273.3}}}{2} \quad (2\text{-}15)$$

where T_{min} and T_{max} are minimum and maximum temperatures, respectively (^oC).

e_a is computed as:

$$e_a = 0.611e^{\frac{17.27\,T_{min}}{T_{min}+273.3}} \quad (2\text{-}16)$$

When available water is more than actual ET, there will be positive correlation between the estimated potential ET and actual ET. A regression analysis of the estimated potential ET on the actual ET can be conducted. This establishes the R^2 (coefficient of determination) indicating the fit between the two sets of data.

2.3.2 Modeling runoff

Inflow to the water balance, or P, was measured using an automatic weather station (WS-STD1, England), installed at the experimental site (Wang *et al.* 2015b). P, initial soil moisture (θ_0), field capacity (θ_{fc}), and wilting point ((θ_{wp}) were used to parameterize the runoff model. The model was calibrated and validated using the observed runoff (Q.) Herein, it was determined that for a 140 cm soil profile, θ_{fc} = 25.6%, θ_0 = 6.7%, θ_{sat} = 46.2%, and θ_{wp} = 6.7% (alfalfa).

The standard SCS – CN method relies on average soil moisture conditions. Soil moisture typical of Gansu Province has a broad moisture range and tends to exceed average soil moisture some times and less than average soil moisture at other times. The SCS – CN method modified to account for changes in soil moisture is outlined by a modified SCS-CN method, called MoCN (Wang *et al.* 2008), expressed as:

$$Q = \frac{(P-I_a)^2}{(P-I_a)+S}; \quad (2\text{-}17)$$

where P = precipitation; I_a = Initial abstraction; S = maximum soil retention after runoff starts.

I_a is computed as:

$$I_a = \lambda \cdot S \cdot \left(\frac{P}{P+S}\right)^{\alpha} \quad (2\text{-}18)$$

where $\lambda = 0.09\ to\ 11.36$, and $\alpha = 0\ to\ 2.82$. λ and α need to be determined by calibration.

S is computed as:

$$S = S_I - M \quad (2\text{-}19)$$

where S_I = maximum soil retention at θ_{wp} and M = reduction of soil retention resulting from increase of soil moisture.

S_I is computed as:

$$S_I = 25.4\left(\frac{1000}{CN_I} - 10\right) \quad (2\text{-}20)$$

where CN_I = curve number at θ_{wp}.

S_{III} is computed as:

$$S_{III} = 25.4\left(\frac{1000}{CN_{III}} - 10\right) \quad (2\text{-}21)$$

where CN_{III} = curve number at θ_{fc}.

M is computed as:

$$M = a \cdot \left(\frac{\theta-\theta_{wp}}{\theta_{sat}-\theta_{wp}}\right)^{b} \quad (2\text{-}22)$$

where θ = current soil moisture, and a and b are two soil-related coefficients.

The two coefficients are computed as:

$$a=S_I \tag{2-23}$$

$$b=\frac{\ln(1-\frac{S_{III}}{S_I})}{\ln(\frac{\theta_{fc}}{\theta_{sat}})} \tag{2-24}$$

The standard SCS – CN method was outlined in the USDA-SCS National Engineering Handbook published in 1973 and modified in 1976 with enhancements to the CN (USDA, 1973). The enhancements yielded CN_I and CN_{II} equations as:

$$CN_I= .39(CN)e^{0.009+CN} \tag{2-25}$$

$$CN_{III}= 1.95(CN)e^{-0.00663+CN} \tag{2-26}$$

where CN = curve number at normal soil moisture condition (i.e., at a soil moisture that is approximately the average of wilting point and field capacity).

CN, λ, and α are variable parameters in the model. The soil moisture θ is estimated in terms of growth phase (Table 2-2) using five-day antecedent precipitation (P_5) as:

$$\theta = \begin{cases} \theta_{wp}\ for\ P_5 < 12.5\ mm\ (dormant\ season)\ or\ P_5 < 35.5\ mm\ (growing\ season) \\ \theta_{wp} + \frac{\theta_{fc}-\theta_{wp}}{15.5} \cdot (P_5 - 12.5)\ for\ 12.5\ mm \le P_5 < 28.0\ mm\ (dormant\ season) \\ \theta_{wp} + \frac{\theta_{fc}-\theta_{wp}}{18.0} \cdot (P_5 - 35.5)\ for\ 35.5\ mm \le P_5 < 53.5\ mm\ (growing\ season) \\ \theta_{fc}\ for\ P_5 \ge 28.0\ mm (dormant\ season) or\ P_5 \ge 53.5\ mm\ (growing\ Season) \end{cases} \tag{2-27}$$

where θ_{wp} = 0.067 (dry soil, AMC_I); $\theta_{fc/sat}$ =0.256 (wet soil, AMC_{III}) for the study site (Wang *et al.* 2015b).

Table 2-2. Definition of alfalfa growing stages.

	Initial Growth	Development Growth	Middle Development Growth	Late Growth	Dormant
Days	10	30	25	10	290
Dates:					
First cut	April 15 to April 24	April 25 to July 4		July 5 to July14	
Harvest	July 15 to July 24	July 25 to October 5		October 6 to October 15	
Growth Season	April 15 to October 15				
Dormant Season	October 16 to April 14 (following year)				

CHAPTER 3

RESULTS AND DISCUSSION

3.1 The Calibrated model

The Loess-like Loam soils of the study region are typically dryer or wetter than the average AMC (Wang *et al.* 2008). Wang *et al.* (2015b) conducted laboratory tests of soil samples at the study site and determined that the wilting point θ_{wp} = 0.067 and the saturated soil moisture θ_{sat} = 0.256. To calibrate the models, three parameters, namely CN, α, and λ, were adjusted simultaneously using Microsoft Excel® Solver to make the modeled monthly runoffs (Q) closely match the corresponding observed values. The upper limit of CN was set to 98, and α was varied from 0 to 5.0 and λ from 0.09 to 11.36. In addition, because the CMR and BMR systems cover the ridges using common plastic mulch and biodegradable mulch, respectively, the maximum retention S (Eq. 2-20) was assumed to be the function of CN only and independent of soil moisture. As a result of the adjustments, the adopted values for these three calibration parameters were determined and are presented in Table 3-1. The values of CN_I, CN_{III}, S_I, and S_{III} for the SR systems are also listed. The corresponding values for the CMR and BMR systems, however, were not used in the models and, thus, are not presented. As expected, the CMR and BMR systems have a larger CN than the SR systems because the ridges of the former systems are covered by mulches. For a given type of system (e.g., SR, CMR, or BMR), the value of α tends to decrease with increase of its ridge width, indicating a smaller initial abstraction I_a (Eq. 2-18).

The calibrated models have good model performances (Table 3-2), as indicated by the slope of the regression lines of modeled monthly runoffs on corresponding observations nearly 1:1, a large R^2 value (> 0.82), and a small root mean square error (RMSE) (< 9.71 mm near the value of minimum P event for crop sustainability). The regression lines are shown in Figures 3-1

to 3-3 for the SR, CMR, and BMR systems, respectively.

Table 3-1. Adopted values of the model parameters.[1]

RFRWH[2]	CN	α	λ	CN_I	CN_{III}	S (mm)	S_I (mm)	S_{III} (mm)
SR^{30}	89	3.26	4.88	78	96	31	73	10
SR^{45}	89	3.40	4.51	78	96	31	73	10
SR^{60}	93	3.65	5.70	83	98	20	51	6
CMR^{30}	97	1.90	0.01			7		
CMR^{45}	97	1.23	0.01			7		
CMR^{60}	98	1.54	0.01			5		
BMR^{30}	97	1.03	0.01			7		
BMR^{45}	97	1.54	0.01			7		
BMR^{60}	98	5.00	0.24			5		

[1] The blank cells signify that these parameters are not related to the BRM and CMR systems.

[2] See Table 2-1 for the ridge and furrow rainwater harvesting systems.

Table 3-2. Summary of the models' performances.

RFRWH[1]	Regression Line[2]	R^2	RMSE (mm)
SR^{30}	y = 0.8898x	0.82	2.51
SR^{45}	y = 0.9211x	0.83	2.89
SR^{60}	y = 0.9979x	0.85	2.98
CMR^{30}	y = 0.9358x	0.88	9.08
CMR^{45}	y = 0.9370x	0.88	8.96
CMR^{60}	y = 0.9381x	0.88	9.71
BMR^{30}	y = 0.9377x	0.89	8.24
BMR^{45}	y = 0.9406x	0.89	8.76
BMR^{60}	y = 0.9416x	0.89	9.11

[1] The blank cells signify that these parameters are not related to the BRM and CMR systems.

[2] Regression of modeled monthly runoffs on responding observations.

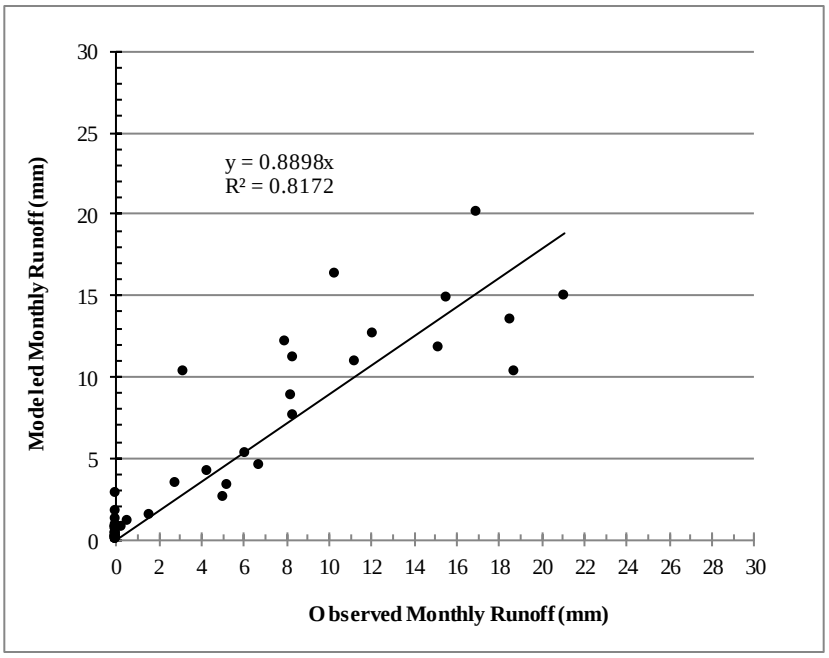
y = 0.8898x
R² = 0.8172
Modeled Monthly Runoff (mm)
Observed Monthly Runoff (mm)
0
5
10
15
20
25
30
0
2
4
6
8
10
12
14
16
18
20
22
24
26
28
30

(a)

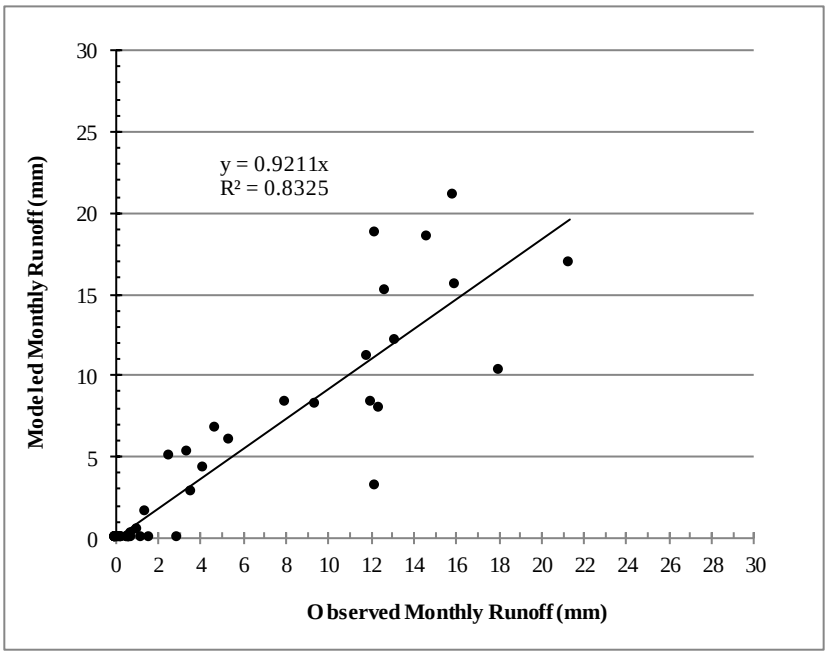
y = 0.9211x
R² = 0.8325
Modeled Monthly Runoff (mm)
Observed Monthly Runoff (mm)
0
5
10
15
20
25
30
0
2
4
6
8
10
12
14
16
18
20
22
24
26
28
30

(b)

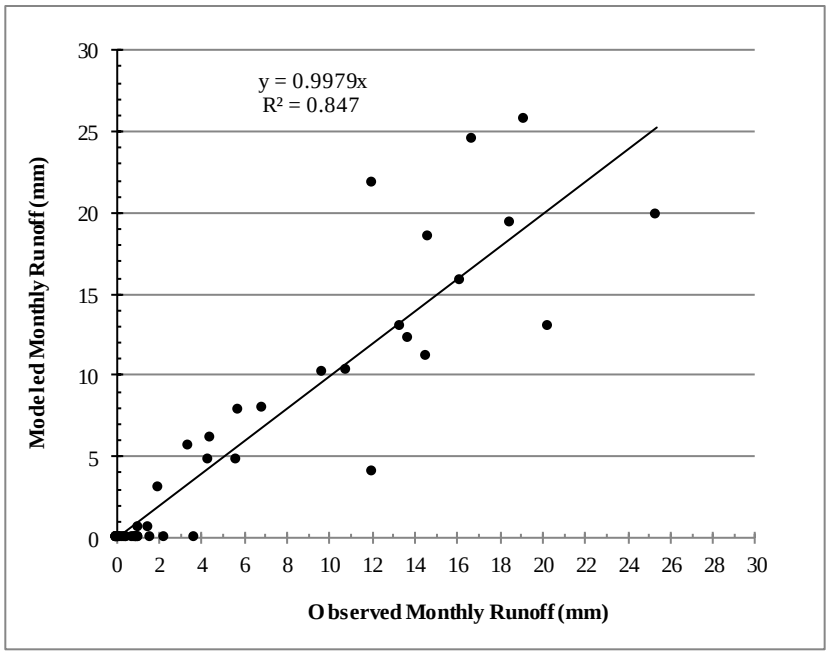

(c)

Figure 3-1. Modeled versus observed monthly runoff for: (a) SR30; (b) SR45; and (c) SR60.

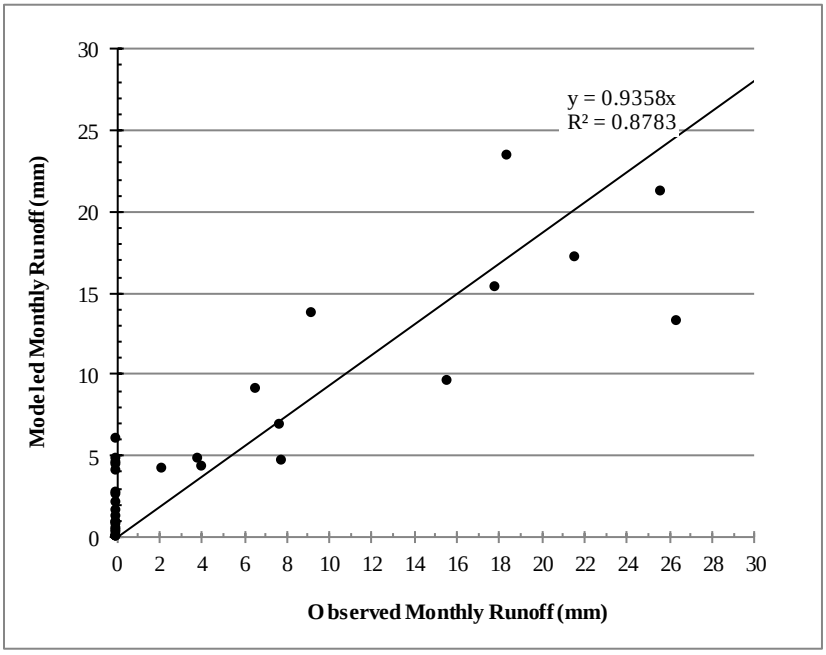

(a)

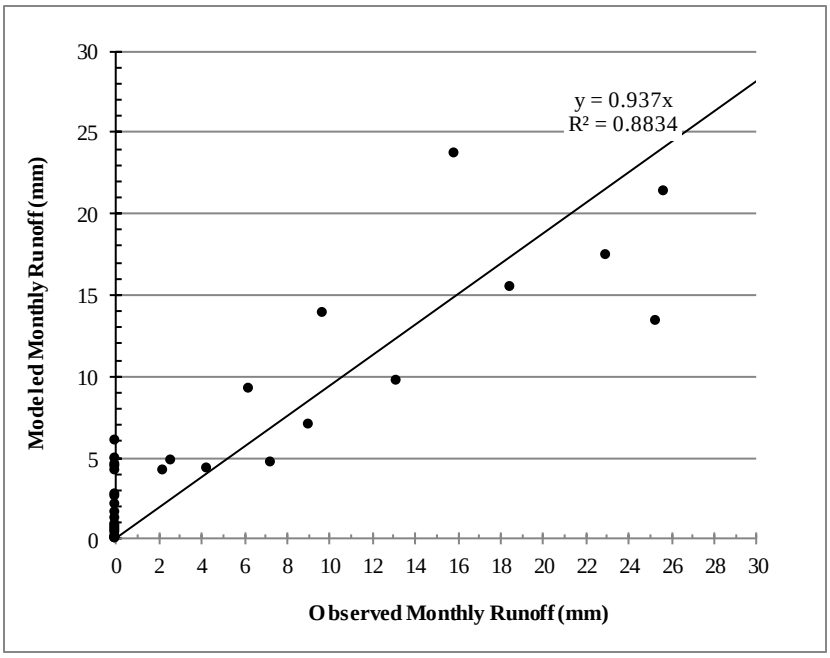

(b)

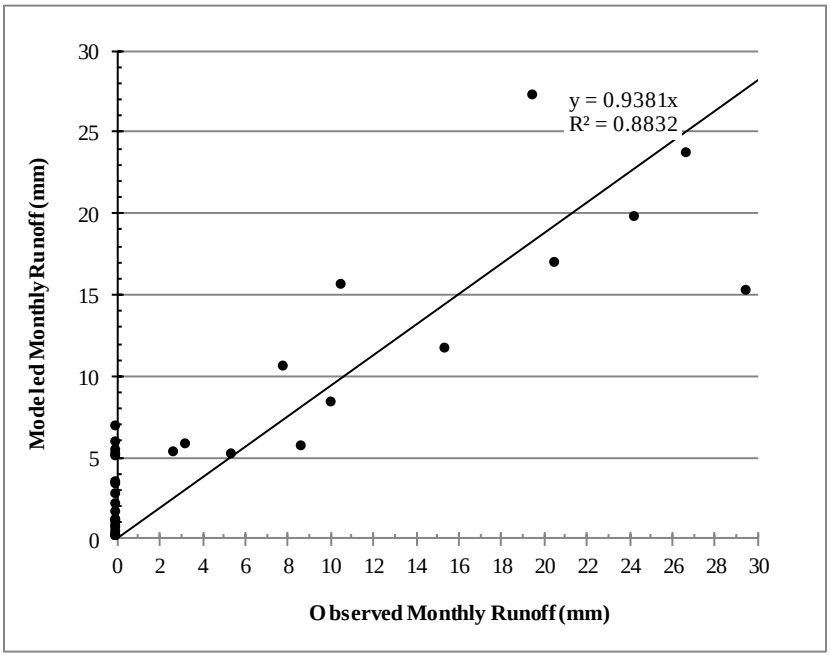

(c)

Figure 3-2. Modeled versus observed monthly runoff for: (a) CMR30; (b) CMR45; and (c) CMR60.

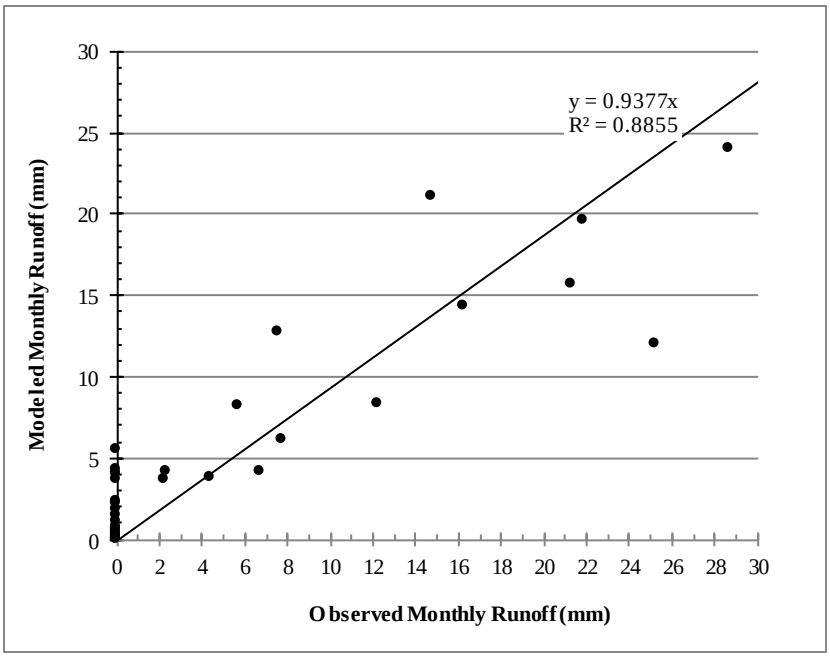
y = 0.9377x
R² = 0.8855
Modeled Monthly Runoff (mm)
Observed Monthly Runoff (mm)
0
5
10
15
20
25
30
0
2
4
6
8
10
12
14
16
18
20
22
24
26
28
30

(a)

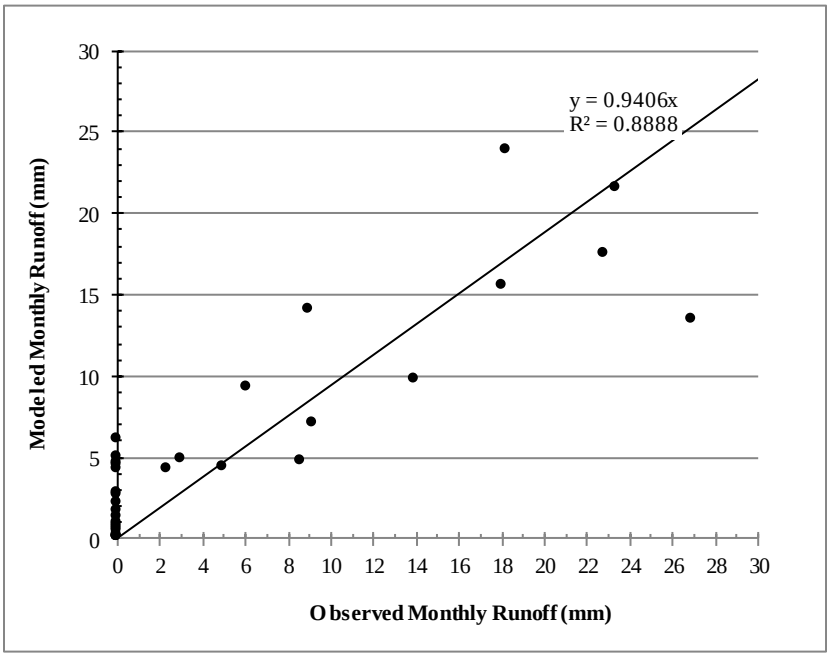
y = 0.9406x
R² = 0.8888
Modeled Monthly Runoff (mm)
Observed Monthly Runoff (mm)
0
5
10
15
20
25
30
0
2
4
6
8
10
12
14
16
18
20
22
24
26
28
30

(b)

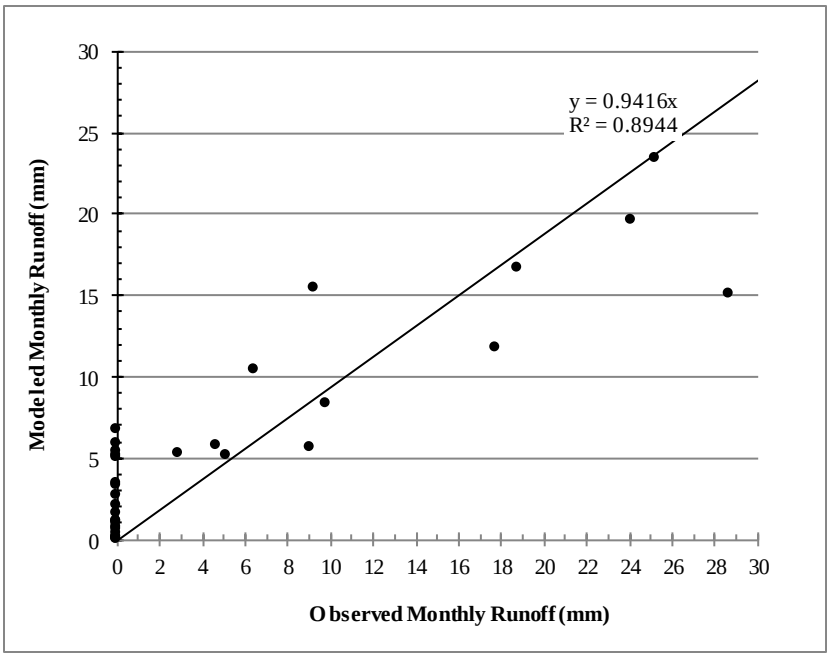

(c)

Figure 3-3. Modeled versus observed monthly runoff for: (a) BMR30; (b) BMR45; and (c) BMR60.

3.2 Simulated Water Yields of the RFRWH Systems

Future climate and its impact on the hydrological cycle is a critical concern for farmers in Gansu Province, China. Water availability affects ecosystems and society. The Gansu Province's annual precipitation is decreasing gradually each year, and 50% of the region's annual precipitation occurs during the months of June to September, a period when many crops are already past the growth stage when they benefit most from precipitation (Wang *et al*. 2015b). Climate change impacts the hydrological cycle by affecting precipitation, surface runoff, and soil moisture (Abu-Allaban *et al.* 2014). Water available from precipitation is expected to decrease 20% or more in the next century (Misra, 2014) due to climate change.

The ridge and furrow rainwater harvesting (RFRWH) model demonstrates higher water yields for crops and designates ordinary precipitation. The climate scenario described and modeled reduces precipitation by 5%, 10%, and 15%. The incremental decreases in precipitation do not reflect actual conditions of precipitation changes; however, it is the simplest way to project possible future changes. The annual average Q_{on} and the average growing season Q_{on} are summarized in Table 3-3 for each model. The use of land cover materials improved Q_{on} in the furrows, with the greatest improvement for the CMR^{60} ridge (Table 3-4). The SR ridges experienced higher water losses, probably due to infiltration and evapotranspiration. Infiltration on the SR ridges was higher than that on BMR and CMR ridges. Additionally, evaporation from the soil surface is greater on SR ridges than CMR and BMR ridges; the land cover provided a means to preserve soil moisture and prevent soil evaporation, improving forage yield. The CMR land cover was the most effective.

Table 3-3. Summary of the simulated mean annual water yields.[1]

RFRWH[2]	Mean Annual Water Yield (mm)				Mean Growing-Season Water Yield (mm)			
	Historical	95%	90%	85%	Historical	95%	90%	85%
SR^{30}	48.87	46.12	44.99	41.60	47.44	44.82	43.82	40.55
SR^{45}	52.45	49.38	47.71	43.47	51.01	48.07	46.53	42.41
SR^{60}	61.99	58.71	57.94	54.01	60.01	56.91	56.31	52.54
CMR^{30}	235.33	219.39	203.65	188.12	226.23	211.01	195.97	181.13
CMR^{45}	237.68	221.63	205.77	190.13	228.45	213.12	197.98	183.03
CMR^{60}	261.77	244.72	227.84	211.17	250.87	234.66	218.59	202.69
BMR^{30}	217.80	202.64	187.70	173.00	209.79	195.29	180.98	166.88
BMR^{45}	238.35	222.27	206.39	190.72	229.06	213.72	198.55	183.58
BMR^{60}	259.32	242.53	225.91	209.47	248.36	232.40	216.59	200.94
	Mean Annual Precipitation (mm)				Mean Growing-Season Precipitation (mm)			
	Historical	95%	90%	85%	Historical	95%	90%	85%
Precipitation	417.87	396.98	376.08	354.99	388.77	369.33	349.89	330.29

[1] Historical: 2012 to 2015; 95%, 90%, and 85%: the daily precipitations in the historical years are reduced by 5, 10, and 15%, respectively.
[2] See Table 2-1 for the ridge and furrow rainwater harvesting systems.

3.3 Simulated Evapotranspiration

Two methods, namely Hargreaves (Eq. 2-3) and FPM (Eq. 2-8), were used to model potential ET. The Hargreaves method is typically used when information available to perform the model is limited to data on maximum and minimum temperature; its required extraterrestrial radiation can be calculated using Eq. (2-4) with inputs of sunset hour, Julian calendar day, and distance between earth and sun. The FPM requires more data, including temperature, radiation, wind speed, and humidity. The FPM calculation procedures are outlined in the FAO 56; a summary of the procedures is provided in Chapter 2 of this thesis. The results of each model and the actual annual ET (Eq. 2-1) are summarized in Table 3-4.

Table 3-4. The modeled annual evapotranspiration.

2012	2013	2014	2015	2016
Potential ET by the FPM method (mm)				
897.43	911.68	953.60	1108.15	1095.11
Potential ET by the Hargreaves Method (mm/day)				
1582.32	1625.57	1632.21	1711.04	1778.48
Measured **A**ctual ET (mm)				
529.78	615.45	466.18	420.99	Missing Data
Percent of Precipitation lost to ET				
95%	85%	98%	70%	

Arid/semi-arid climates typically have the annual potential ET greater than annual precipitation. In the Gansu Province average annual precipitation from 2012 to 2016 data was 417.87 mm, while the average annual potential evapotranspiration (PET) was 1665.92 mm using the Hargreaves method and 993.19 mm using the FPM method. The precipitation lost to ET ranged from 70 to 95%. The two components for ET are soil evaporation and crop transpiration. The RFRWH system improvements reduce evaporation from the soil, and as crop cover increases during the growing seasons, transpiration from the crop surface increased. The modeled PET and the measured actual ET cannot be correlated because of the short record period (only four years). Nevertheless, both models indicate that PET tended to increase in past years possibly due to climate change. In terms of the FAO 56 crop coefficient for alfalfa of 0.40, it was estimated that the average soil evaporation during the growing seasons was reduced by 40% decrease due to the RFRWH systems. This reduced soil evaporation increased the water available for crops in the furrows, increasing crop yields. Overall, it seems that the percentage of precipitation lost to total evapotranspiration can be reduced by using the RFRWH systems, as indicated by the values in Table 3-4.

3.4 Summary and Discussion

The Gansu Province of China is characterized by a climate that experiences heavy and sporadic storms for a short period followed by long periods of drought. Global warming and climate change are the main causes of the sporadic rainfall patterns (Wang *et al*. 2015b). RFRWH in arid/semi-arid regions helps farmers optimize irrigation by storing and using Q_{on} from rainfall events to supply water needed for agriculture during drought periods. Many of the regions that implemented RFRWH practices showed increases of soil moisture and yields for various crops native to the particular region (Wang *et al.* 2015b).

The soil moisture in arid/semiarid regions such as the study site of this thesis usually has a large temporal variation due to non-beneficial evaporation of soil water. Given that soil water is the primary water source for crops in such regions, it is important to use measures like RFRWH systems to reduce non-beneficial evaporation and increase water yield for irrigation during the growing season. In this regard, quantifying effects of the RFRWH is needed for designing and implementing most effective measures. This thesis calibrated and used a MoSCS-CN model to assess the effects of six selected RFRWH systems, namely SR^{30}, SR^{45}, SR^{60}, CMR^{30}, CMR^{45}, CMR^{60}, BRM^{30}, BRM^{45}, and BMR^{60} (Table 2-1). The model has a very good performance (Table 3-2 and Figures 3-1 to 3-3). The CMR^{60} was predicted to have the highest water yield, implying an increased soil moisture and possibly a higher forage yield since there will be more water available to nourish the crop within the furrows. The BMR covers were predicted to be slightly less effective than the CMR covers, whereas the SR systems were predicted to be least effective.

A summary of the results of the potential ET predicted by the Hargreaves and FPM methods as well as the measured actual ET is provided in Table 3-4. Although a correlation

analysis between PET and actual ET was impossible because of the short record period (only four years), the results clearly show an increasing trend of PET probably caused by warming climate and the reduction effects of the BMR and CMR covers on non-beneficial soil water evaporation. It is recommended that more data be collected in the future to differentiate the effects of the BMR and CMR covers in reducing soil evaporation while increasing crop transpiration. Also, a crop model may be coupled with the MoSCS-CN and ET models to better mimic the dynamic water-soil-crop interactions.

CHAPTER 4

CONCLUSIONS AND RECOMMENDATIONS

4.1 Conclusions

The water balance (Eq. 1-1) is an important tool for water resource planners to implement irrigation practices in arid/semiarid regions using water harvested by using ridge and furrow rainwater harvesting (RFRWH) systems. Agriculture in Gansu Province of China is vulnerable because of the changing climate that is characterized by sporadic rainfall events followed by long-lasting non-rainy days. As a result, extreme water shortages and localized instantaneous heavy storms with a duration of less than several minutes are prevalent. Alfalfa, which is the concerned crop of this study, has a growing season from April through October, but most of the rainfall occurs from June through September, making the crop short of water during its crucial initial stages (April and May) of seedling, germination, and emergence. These two beginning months are usually very dry with a soil moisture near the wilting point. In this regard, various types of RFRWH systems have been practiced/constructed in the province as well as many other regions with similar climate conditions to provide a means to supply water needed during early growing stages by storing excess water from sporadic heavy storms. In addition to regulating the temporal distribution of water availability, the RFRWH systems can also replenish soil moisture and reduce non-beneficial evaporation from bare soils.

This thesis developed hydrologic models to predict effects of the RFRWH systems on water yield increase and non-beneficial evaporation reduction. The water yield increase was modeled using the MoCN method with curve number varied with soil moisture and/or mulch materials of ridges. Herein, the systems studied have three types of ridge covers, namely soil crust (SR), common plastic mulch (CMR), and biodegradable plastic mulch (BMR). In addition,

each of the systems has three ridge widths of 30, 45, and 60 cm. In total, nine groups of RFRWH systems, namely SR^{30}, SR^{45}, SR^{60}, BMR^{30}, BMR^{45}, CMR^{45}, CMR^{30}, BMR^{60}, and CMR^{60} were modeled. The models were calibrated using the observed monthly runoffs from 2012 to 2015 and are judged to have good performances, as indicated by large values of coefficient of determination ($R^2 > 0.82$) and small values of root mean square error (RMSE < 9.71 mm). This good performance was also verified by visualization plots showing the modeled versus observed monthly runoff.

The effects of the RFRWH systems on water yield increase were evaluated for three scenarios of precipitation, including the historical, 5% reduction, 10% reduction, and 15% reduction. The results indicate that regardless of the precipitation scenarios water yield was predicted to increase with increase of ridge width and that for a given precipitation scenario the CMR^{60} system was predicted to have a highest water yield. The BMR^{60} system was predicted to have a slightly lower increase of water yield than the CMR^{60} system. Overall, these two systems may be good choices for increasing water availability and adapting to climate change.

On the other hand, the effects of the RFRWH systems of evapotranspiration (ET) were modeled using the Hargreaves model (Eq. 2-3) and the FAO Penman Monteith (FPM) model (Eq. 2-7). These two models predict potential ET, which is the maximum amount of water needed to satisfy the climatic demand under given climate conditions. Although the modeled PET and the measured actual ET cannot be correlated because of the short record period (only four years), both models indicate that PET tended to increase in the last few years possibly due to climate change. In terms of the FAO 56 crop coefficient for alfalfa of 0.40, it was estimated that the average soil evaporation during the growing seasons was reduced by 40% due to the RFRWH systems. This reduced soil evaporation might have increased the water available for

crops in the furrows, increasing the crops yields. Overall, it seems that the percentage of precipitation lost to non-beneficial soil evaporation is likely to be reduced by up to 30% (Table 3-4) from using the RFRWH systems.

In conclusion, the RFRWH systems can be a cost-effective means to increasing surface water yield, replenishing soil water, regulating temporal distribution of water availability, reducing non-beneficial evaporation from bare soils, and thus sustaining the agricultural productivity and eco-environment in arid/semiarid regions such as Gansu Province of China.

4.2 Recommendation for future Research

The RFRWH systems that were studied by Wang *et al*. (2015b) showed positive effects on water yield. The study concluded that the systems will increase soil moisture, reduce impacts of changing temperature and water availability on agriculture, and increase crop yield. While there are historical weather data on temperature and precipitation, data on runoff and ET are scarce. The data on actual ET data are not long enough to do a trend analysis, making it uncertain whether ET has been increasing or decreasing. Although this thesis detected an increasing trend of PET, the models' performances could not be validated because observed data were not available. In addition to collecting more data on PET and actual ET, it is recommended to improve the models to reflect how soil heat flux is affected by various mulches.

REFERENCES

Adham, A.; Riksen, M.; Ouessar, M.; Ritsema, C. (2016). Identification of suitable sites for rainwater harvesting structures in arid and semi-arid regions: A review. *International Soil and Water Conservation Research,* 4(2): 108-120.

Abu-Allaban, M.; El-Naqa, A.; Jaber, M.; Hammouri, N.(2014). Water Scarcity Impact of Climate Change in Semi-Arid Regions: A Case Study in Mujib Basin, Jordan. *Arabian Journal of Geoscience*, 8:951-959.

Allen, R.G; Pereira, L.S.; Raes, D.; Smith, M. (2006). " FAO Irrigation and Drainage Paper No. 56," Federal Agriculture Organization.

Feser, F.; Rockel, B.; Storch, H.V.; Winterfeldt, J.; Zahn, M. (2011). Regional Climate Models Add Value to Global Model Data. A Review and Selected Examples. *Bulletin of the American Meteorological Society*, 92(9):1181-1192

Hargreaves, G.H.; Allen, R. (2003). History and Evaluation of Hargreaves Evapotranspiration Equation. *Journal of Irrigation and Drainage Engineering*. 129:53-63.

Helmreich, B.; Horn, H. (2008). Opportunities in Rainwater Harvesting. *Desalination,* 248:118-124

Huang, M.; Gallichand, J.; Wang, Z.; Goulet, M. (2005). A Modification to the Soil Conservation Service Curve Number Method for Steep Slopes in the Loess Plateau of China. *Hydrological Processes Journal* 20(2006):579-589.

Kumar, R; Shankar, V; Kumar, M (2011). Modeling of Crop Reference Evaporation: A review. *Universal Journal of Environmental Research and Technology*. 1:239-246.

Misra, A.K. 2014. Climate Change and Challenges of Water and Food Security. *International Journal of Sustainable Built Environment* 3(1): 153-165.

Mishra, S. K., Jain, M. K., and Singh, V. P. (2004). Evaluation of SCSCN-Based Model Incorporating Antecedent Moisture. *Water Resource Management*, 18(6), 567–589.

United States Department of Agriculture (USDA) SCS - National Engineering Handbook (1973)

Shi, Z.; Xu, L.; Yang, X.; Guo, H.; Dong, L.; Song, A.; Zhang, X.; Shan, N.;(2016). Trends in Reference Evapotranspiration and its Attribution over the Past 50 Years in the Loess Plateau, China: Implications for Ecological Projects and Agricultural Production. *Stochastic Environmental Research and Risk Assessment*, 31:257-273.

Su, X.; Singh, VP; Niu, J; Hao, L; (2015). Spatio-Temporal Trends of Aridity Index in Shiyang River Basin of Northwest China. *Stochastic Environmental Research and Risk Assessment*, 29:1571–1582.

Wang, X.; Shang, W.;Yang, W.; Melesse, M. (2008). Simulation of an Agricultural Watershed Using an Improved Curve Number Method in SWAT. *American Society of Agricultural and Biological Engineers*, 51(4):1323-1339.

Wang, G.; Shang, J.; Jin, j.; Weinberg, J; Bao, Z, Liu C.; Liu, Y.; Yan, X; Song, X.; Shai, R. (2015a). Impacts of climate change on water resources in the Yellow River basin and

identification of global adaptation strategies. *Mitigation Adaptive Strategies Global Change*, 22:67-83.

Wang, Q; Xiang, R.; Xingyang, S.; Guangrong, H.; Enhe, Z.; Heling, W.; Vance, M. (2015b). The Optimum Ridge – Furrow Ratio and Suitable Ridge Covering Material in Rainwater Harvesting for Alfalfa Production in Semiarid Regions of China. *Field Crops Research Journal* 180: 186-196.

Zhao, C.; Feng, Z.; Chen, G.; (2004). Soil Water Balance Simulation of Alfalfa (medicago sativa L.) in the Semiarid Chinese Loess Plateau. *Agricultural Water Management*, 69:101-114.

VITA

Tennille Wade PE

Experience summary:
10 years' experience with water resources engineering specialized in stormwater, water, and wastewater design and construction. Public and private sector experience.

Education History
Old Dominion University
BS Civil Engineering w/ a Minor in Engineering Management (2009)
MS Environmental Engineering (May 2018)

Technical Proficiency
AutoCAD Civil 3d, Arc GIS, Microsoft Word, Excel, Access, Micro station V8 and Power Point.

Experience
City of Newport News July 2016- Present
Full-time Project Manager Position
Manage all budget, design, and construction for wastewater, and stormwater projects.

WSP Parsons Brinckerhoff November 2014 – July 2016
Full-time Engineer II Position
Designed large and small diameter water pipeline projects, and sanitary force mains.

City of Petersburg August 2013- October 2014
Full-time City Engineer Position
Managed engineering projects in Petersburg.

O'Brien & Gere Engineers May 2009- August 2013
Full-time Design Engineer Position
Entry level design engineer prepared design plans for water and sanitary sewer projects.

Clark Nexsen Engineers June 2005- March 2007
Full-time CADD Technician Position
Provided drafting support to engineers for site development projects.

MSA P.C. Nov 2003- June 2005
Full-time Land Planner Position
Provided site development design support to landscape architect.

US Air Force June 1999- Oct 2003
Full-time Engineering Aid Position